



Preparation, characterization and absorption of Li_2MnO_3 - carbon – poly(vinylidene fluoride) nanocomposites for lithium-ion batteries under different pH level

Zainab R.Muslim¹, Ali Q. Kadhum¹, Zina A. Al Shadidi², Smah A.Kadhum¹

¹College of Science, University of Baghdad, Baghdad, Iraq

²Department of Radiology /Al Ma'moun University College /Baghdad/Iraq

*) Email: zainabraheem2018@ahoo.com

Received 21/10/2024, Received in revised form 3/12/2024, Accepted 9/12/2024, Published 15/2/2025

Transition-metal layer Li_2MnO_3 (LMO) prepared using the Sol-Gel process for use in energy systems as cathode in Li- ion batteries. Structural properties are studied for LMO powders using Diffraction of Xrays (XRD). The findings suggest that a crystalline monoclinic phase is displayed during the production of LMO. Atomic Force Microscopy (AFM) shows that the average diameter is 45.71 nm for LMO. Scanning Electron Microscopies (SEM) for LMO shows uniform spherical structures. The thermal analysis is done by using thermo-gravimetric analysis (TGA), revealed that LMO is thermally stable, the melting temperature is 912.96°C and the crystallization temperature is 295.41°C. The aim of this study is to enhance the absorption of electrodes by the variation of pH by Electrodes absorption measurement for LMO with different percentages of PVDF and activated carbon are measured, LMO nanocomposites shows higher ability to absorb in acidic solutions.

Keywords: Preparation; Absorption; Nanocomposites.

1. INTRODUCTION

Nanostructures have shown greater promise for a range of uses because of the unique characteristics triggered at small particle sizes. [1-5]. The main requirement for the high mileage of electric vehicles is always a huge battery capacity. The capacity of lithium-rich layered oxides (LLOs) is greater than that of conventional cathode materials (LiTMO_2 , where TM = transition metal). However, after the first cycle, the capacity attenuation of LLOs remains a constraint. Consequently, a thorough investigation of the oxidation mechanism of Li_2MnO_3 , the primary constituent of Li-rich cathode material, at highly charged states is required [6-8].

Compared to cobalt oxide, which is used in the majority of Li-ion batteries, they are less expensive and toxic while still offering high-rate capabilities and good specific capacities [8-12].

2. PREPARATION OF Li_2MnO_3

To create LMO, the "Sol-gel process" is employed. (10)g of salt-form citric acid is weighed on a single pan balance, dissolved in the necessary volume of deionized water, and vigorously mixed. Three distinct beakers are filled to stoichiometric levels with LiNO_3 , manganese acetate, and citric acid in a ratio of 1:1:2. Citric acid is added drop by drop. The obtained standardized solution is thoroughly stirred in a magnetic stirrer at (80–90) °C for four to six hours, or until gel formation, in order to remove the excess water. The gel-filled beaker is first cooked in a hot air oven for 12 hours at 150 °C. It is then heated in an oven for 6 hours at 700 °C.

3. RESULT AND DISCUSSION

3.1 X-Ray Diffraction Analysis for Lithium manganese oxide Li_2MnO_3

The X-ray diffraction spectra pattern for a LMO is displayed in Figure (1) which shows X-ray diffraction spectra of LMO at 150 °C. It shows monoclinic crystal structure peaks powder sample at 700 °C which identified for reation of a monoclinic structure that closely resembles powder LMO data from the International Center of Diffraction Data Card (ICDD). Corresponding to the planes (001), (110), (11-1), (021), (130), (131), (-132), (132) and (-133), in accordance with an approach describing the monoclinic LMO structure [13].

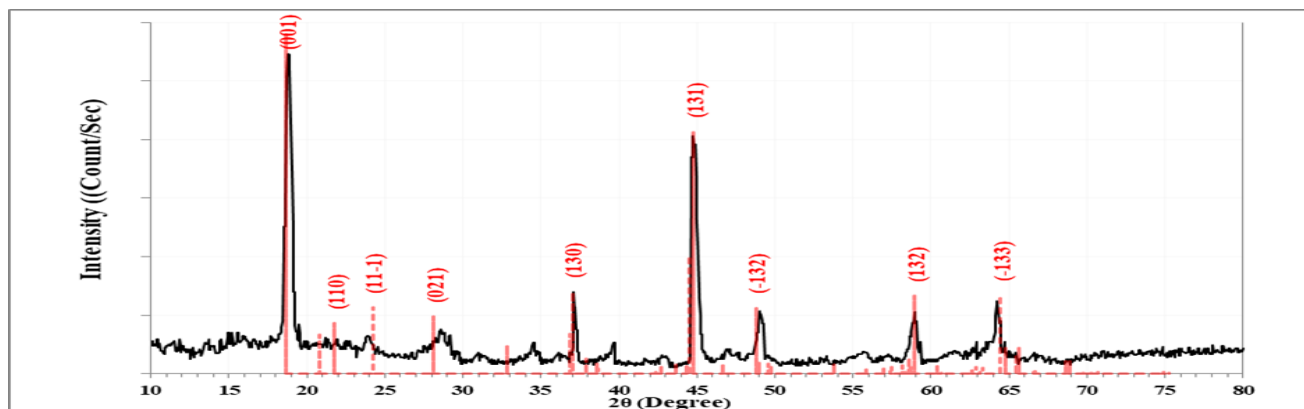


Figure 1 XRD for LMO.

3.2 Atomic Force Microscopy (AFM) of Li_2MnO_3

The AFM images for the surface of the LMO are shown in Figure (2). The pictures are shown a uniform surface; indicating that the particle has uniform dimensions, 3D pictures with a Z range exaggeration to highlight the sample's characteristics. It is discovered that the average surface diameter for LMO is 45.71 nm.

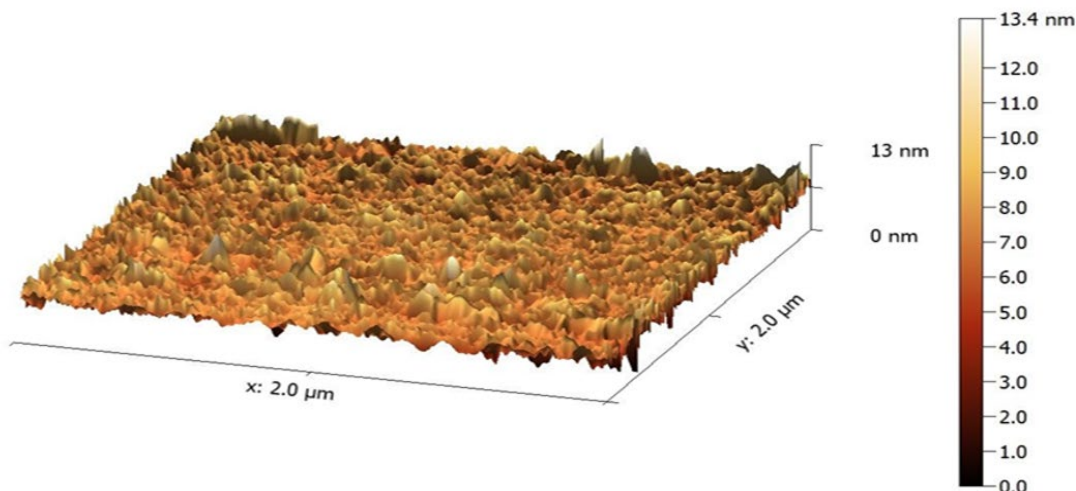


Figure 2 AFM micrograph of LMO in 3D.

3.3 Scanning Electron Microscope Results of Li_2MnO_3

The SEM image of LMO powder shown in Figure (3) which indicate that the particles are flakes [14-17].

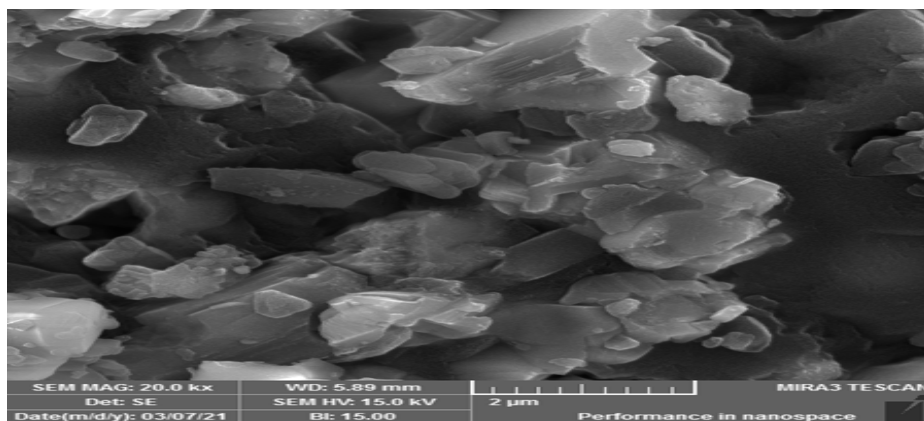


Figure 3 SEM image of LMO powder.

3.4 Thermo-Gravimetric Analysis (TGA) of Li_2MnO_3

There are four regions to the sample's weight reduction due to dehydration, dehydroxylation, and decarburization with the rearrangement of material structure at various temperatures as the first noticeable weight loss happens between 45°C and 135°C, and it may be related to the release of water that has been adsorbed, Fig. 4. The following weight loss happens between 135°C and 250°C, and it can be brought on by the precursors' constituents burning and disintegrating. Between 250°C and 350°C, there is another zone of weight loss that could be caused by the breakdown of precursor material, the burning of the gelling agent, and the creation or crystallization of LMO. The next weight loss occurs between 350°C and 580°C. Above 500°C

There isn't a noticeable shift in weight that would suggest LMO development.spinel, which is stable afterward [13,14].

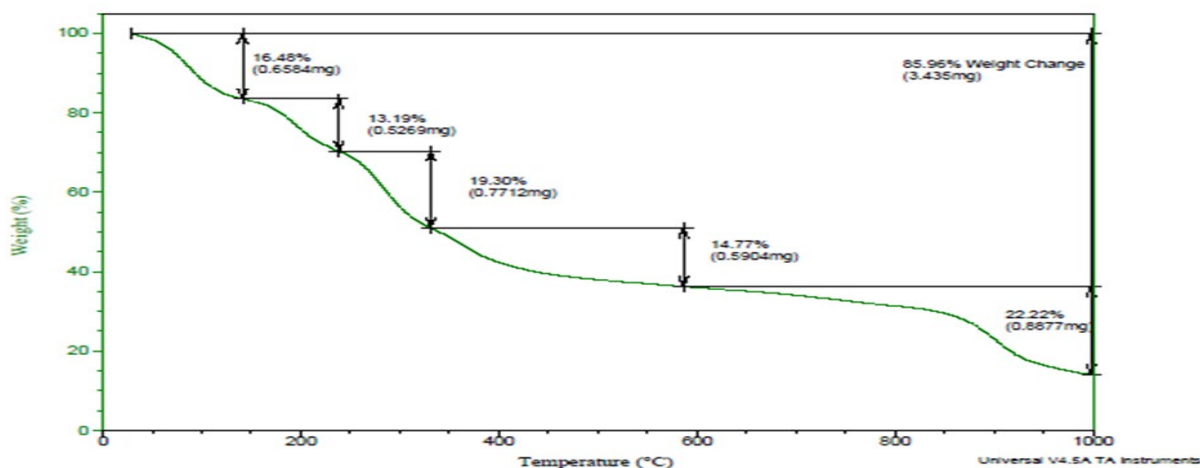


Figure 4 Thermo-gravimetric curve of LMO.

3.5 Electrodes Absorption Results of Li_2MnO_3

Figures (5), (6), and (7) shows the effect of the absorbance of solutions on LMO samples with different percentages of PVDF and activated carbon. The results illustrated the water absorption increases with time and the weight gain for all mixtures increased, the highest value, which is for the acidic solution because the weight of PVDF increases due to the hydrophobicity of polymer. The highest absorption is observed in the base solution while the lowest one is in the acid solution in the sample, which contained 50% LMO and 50% PVDF because acids seem to have minimal effect on PVDF because metals with a positive standard reduction potential will not react with acids under normal conditions. Also, synthetic polymers can be hydrolyzed by strong acids though these tend to react more slowly.

An acid is a substance that donates hydrogen ions into a solution, while a base or alkali takes up hydrogen ions. Due to the relatively higher stability of the passive layer at basic pH, most metals have a lesser tendency for corrosion in bases compared to acids and vice versa. By selecting an appropriate electrode material and learning about the electrochemical behavior of various types of electrode materials at pH 2, 7, and 9, electrochemical phenomena at electrode/solution interfaces during heating can be avoided or efficiently prevented. The diffusion properties for lithium-ion (Li-ion) batteries, the performance of the positive and negative electrodes is investigated. The microstructure of electrodes is primarily determined by manufacturing processes, which also have an impact on the active materials' participation in electrochemical reactions. The increase in activated carbon act as a bridging cause to interfere in pores in PVDF and oxides leading to lower weight gain, the higher weight gain (ratio 50% PVDF) is attributed to higher pores which act as a diffusor ion transfer.

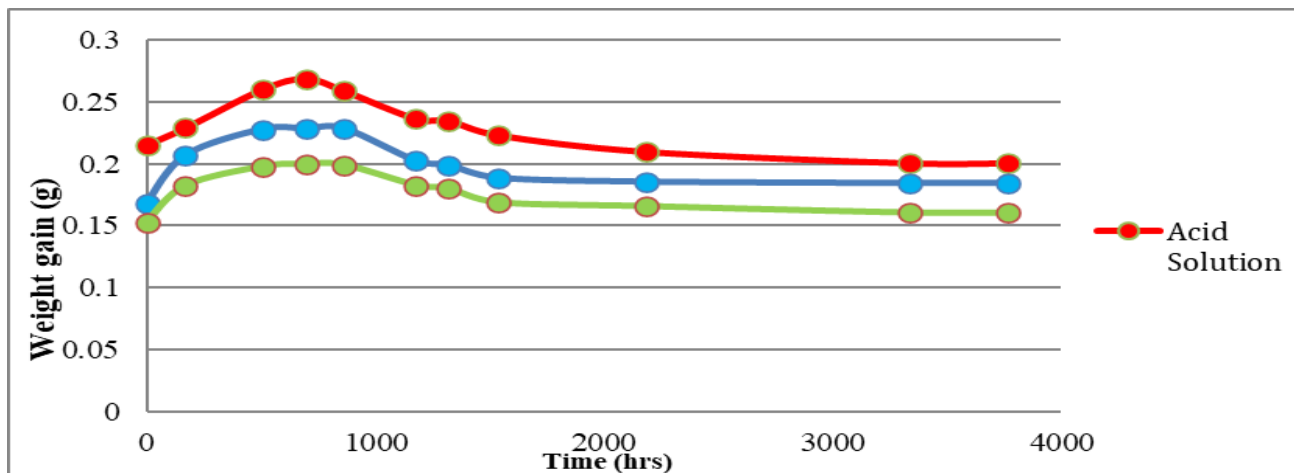


Figure 5 Weight gain as a function of time at ratio 20% PVDF and 30% (AC) added to LMO.

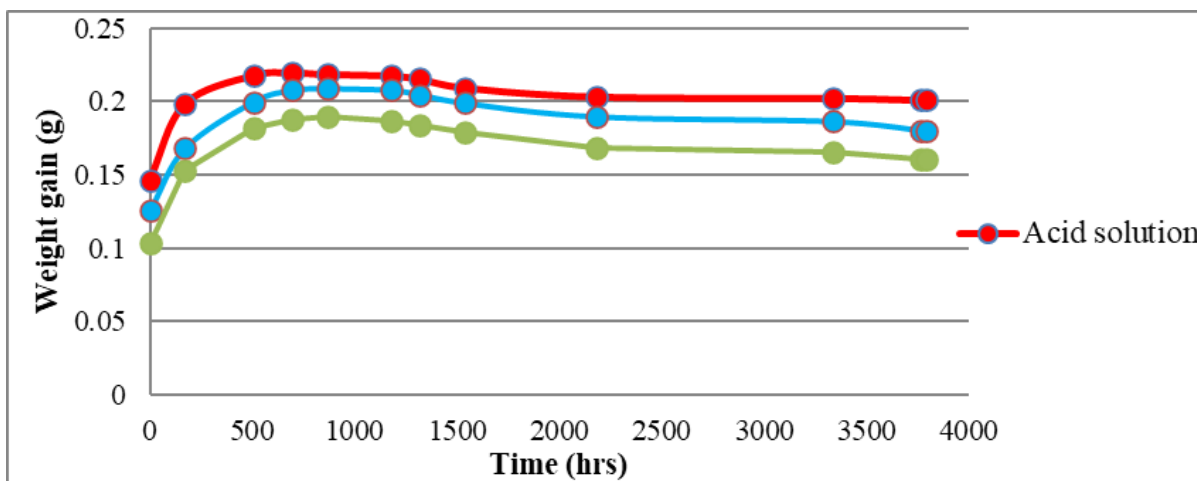


Figure 6 Weight gain as a function of time at ratio 30% PVDF and 20% (AC) added to LMO.

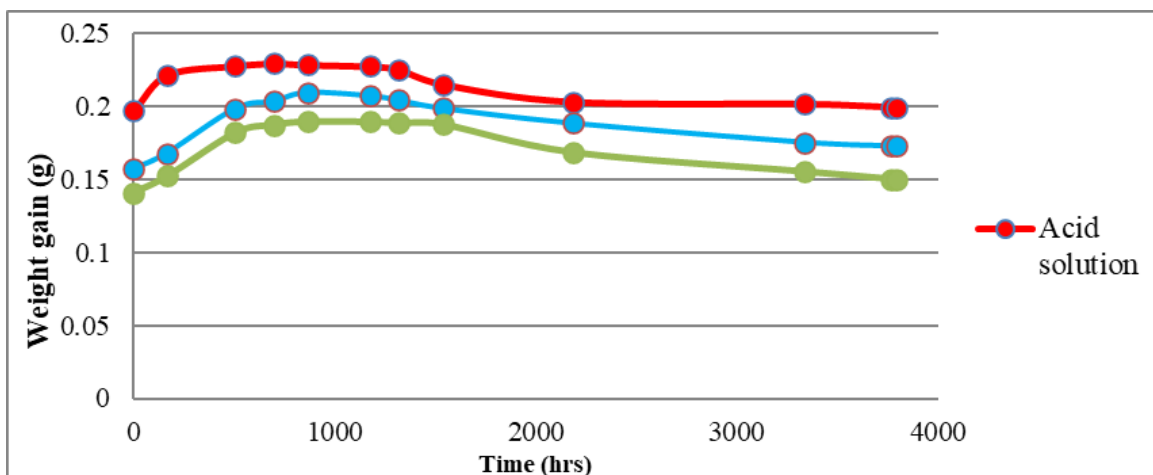


Figure 7 Weight gain as a function of time at ratio 40% PVDF and 10% (AC) added to LMO.

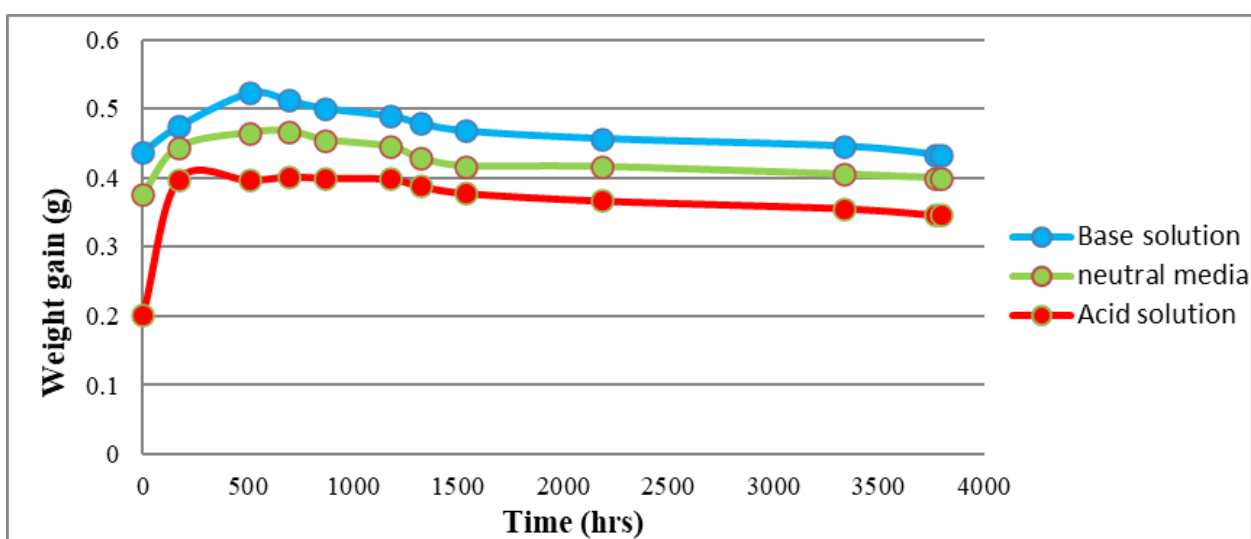


Figure 8 Weight gain as a function of time of LMO at ratio 50% PVDF.

4. CONCLUSIONS

Absorption Results of LMO samples with different percentages of PVDF and activated carbon, shows that LMO the higher ability to absorb in acidic solutions.

References

- [1] J. Radehaus, Exp. Theo. NANOTECHNOLOGY 7 (2023) 143
- [2] E. Hossain, H.M.R. Faruque, M.S.H. Sunny, N. Mohammad, N. Nawar, Energies 13 (2020) 3651
- [3] H. Wang, J. Zhang, X. Hang, X. Zhang, J. Xie, B. Pan, Y. Xie, Angew. Chem. 127 (2015) 1211
- [4] M.M. Najafpour, I. Zaharieva, Z. Zand, S.M. Hosseini, M. Kouzmanova, M. Hołyńska, S.I. Allakhverdiev, Coord. Chem. Rev. 409 (2020) 213183

- [5] D.P. Dubal, D.S. Dhawale, R.R. Salunkhe, C.D. Lokhande, *J. Electrochem. Soc.* 157 (2010) A812
- [6] S.C. Pang, M.A. Anderson, *J. Mater. Res.* 15 (2000) 2096
- [7] S.I. Hussein, N.A. Ali, A.S. Khalil, Z.R. Muslim, M.K. Jawad, *AIP Conf. Proc.* 3229 (2024) 070017
- [8] Z.R. Muslim, A.Q. Kadhum, *J. Phys. Conf. Ser.* 1591 (2020) 012005
- [9] M.K. Jawad, F.T.M. Noori, S.I. Hussein, N.A. Ali, Z.R. Muslim, M.A. Saleh, *Iraqi J. Appl. Phys.* 20 (2024) 3
- [10] M.M. Thackeray, C.S. Johnson, J.T. Vaughey, N. Li, S.A. Hackney, *J. Mater. Chem.* 15 (2005) 2257
- [11] A.M. Hammed, Z.R. Muslim, *Mater. Sci. Eng.* 928 (2020) 1
- [12] R. Fouad, Z.R. Muslim, *J. Phys. Conf. Ser.* 1879 (2021) 032066
- [13] R. Fouad, Z.R. Muslim, *J. Phys. Conf. Ser.* (2020) 1
- [14] F. M., D. Djamel, A. Ch., L. H., T. Touam, *Arab J. Basic Appl. Sci.* 27 (2020) 423
- [15] Abraham George, *Exp. Theo. NANOTECHNOLOGY* 8 (2024) 1
- [16] M. Tadres, *Exp. Theo. NANOTECHNOLOGY* 8 (2024) 11
- [17] J. G. Kim, P. Tan, *Exp. Theo. NANOTECHNOLOGY* 8 (2024) 17

